Analyzing Nonexponential Kinetics with Multiple Population-Period Transient Spectroscopy (MUPPETS)

Champak Khurmi and Mark A. Berg*

Department of Chemistry and Biochemistry, University of South Carolina, Columbia, South Carolina 29208

Received: November 8, 2007; In Final Form: January 29, 2008

A new multidimensional spectroscopy (MUPPETS) was recently introduced (van Veldhoven, E.; et al. *ChemPhysChem* **2007**, *8*, 1761) that distinguishes between nonexponential relaxations that are due to heterogeneous dynamics and those that are due to homogeneous dynamics. This paper develops methods for the quantitative analysis of MUPPETS data and demonstrates the ability of this experiment to decompose a complex decay into its components. These methods have been applied to MUPPETS data on the ground-state recovery of auramine in methanol and on a mixture of auramine and coumarin 102 in methanol. The auramine is found to have two kinetically different components, even though the decay times are too similar to be distinguished in a one-dimensional experiment. The dynamics of each component are derived from the MUPPETS data in a model-free procedure in particular without assuming that the individual decays are exponential or that they have similar shapes. In fact, the component decays are each found to be nonexponential and to have different decay shapes. We suggest that the two components are due to ion-paired and nonpaired molecules. The effect of rotation on MUPPETS with all parallel polarizations is analyzed. The nonexponentiality in ground-state recovery signals due to the combination of rotation and population decay is shown to behave as a nearly ideal homogeneous nonexponentiality. This prediction is confirmed in a mixture of auramine and coumarin. MUPPETS allows the decay from the fast relaxing auramine to be removed from the mixture, leaving only the rotation/population decay of the coumarin.

Introduction

A single-exponential decay is the simplest and most common form for many different relaxation processes in many different systems. However, in complex systems nonexponential decays are also frequently found. An easy explanation of the nonexponentiality is that the sample consists of two or more subensembles, each with an exponential decay but each with a different rate. In other words, the sample is dynamically heterogeneous.[1,2] On the other hand, it is possible to devise plausible mechanisms in which the first part of the decay occurs at an inherently different rate than later portions. Because each individual molecule undergoes the same nonexponential relaxation, such mechanisms can be called dynamically homogeneous. In conventional experiments that use only one time dimension, these two types of nonexponential decay cannot be distinguished. This paper develops the analysis of a new two-dimensional experiment that discriminates between these different causes of nonexponential relaxation.[3]

Why is a new experiment needed? In favorable situations, heterogeneity can be detected by characteristics independent of the relaxation itself: different chemical species can be physically separated, or different dynamic subensembles may have distinct spectra. Yet in many situations, dynamic heterogeneity is more difficult to detect. The different subensembles may exchange on a time scale slower than the observed relaxation process, but still fast enough to frustrate physical separation, or the subensembles may not have distinguishable spectra. Examples of these difficult-to-measure heterogeneities include protein substates,[4] DNA conformations,[5,6] solvent−solute complexes, or local structures in materials such as supercooled liquids,[2] polymers[7] or bilayers.

Single-molecule spectroscopy can be a powerful tool in these circumstances.[8] However, no more than one photon can be collected for each relaxation cycle of a single molecule, and many photons are needed to measure an instantaneous rate. As a result, single-molecule spectroscopy is restricted to relatively long-lived heterogeneities.

On the other hand, one cannot always assume that a nonexponential relaxation is caused by heterogeneity. For example, a molecule in an excited electronic state can undergo conformational relaxation or solvation following excitation. If these processes change the decay rate of the excited state, the rate is inherently time-dependent. The same nonexponential decay would be observed for every individual molecule in the sample. Another example is rotation of a solute in a locally structured material, such as a micelle. The solute can wobble rapidly through a small cone of angles relative to the local micelle structure, but complete reorientation requires diffusion of the solute around the micelle.[9] The same two phases of relaxation occur for every solute molecule.

Thus, when confronted with a nonexponential decay two questions must be answered: Is the decay homogeneous or heterogeneous? And if the decay is heterogeneous, what are the relaxation properties of each individual component?

We recently introduced a new approach to answering these questions, which we call *Mu*ltiple *P*opulation *Pe*riod *T*ransient *S*pectroscopy (MUPPETS).[3,10] It is a type of two-dimensional spectroscopy in which relaxation during different time periods is compared. Unlike other two-dimensional spectroscopies,[11−15] it compares the decay of population during these periods, not

* To whom correspondence should be addressed. Phone: 803-777-1514. E-mail: berg@mail.chem.sc.edu.

10.1021/jp710711w CCC: $40.75
Published on Web 03/08/2008

CHART 1: Chemical Structures of the Two Dyes Used in This Paper

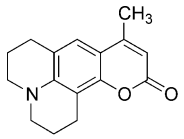

Coumarin 102

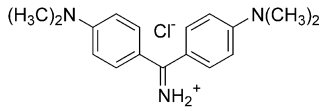

Auramine

the oscillation of coherences. MUPPETS answers the following question: If a molecule relaxes more rapidly than the average after one excitation, will it also relax rapidly after a second excitation? If the decay is heterogeneous, the answer will be yes. If the decay is homogeneous, the answer will be no. The determination of dynamic heterogeneity is made only on the basis of the relaxation itself; no associated spectral changes are required. The heterogeneity only needs to have a lifetime longer than the relaxation process being measured.

Previous examples of experiments that use multiple population excitations are relatively few, but they have appeared sporadically in the literature for a variety of purposes: stimulated-emission pumping has been used to excite high vibrational states;[16,17] Schwartz has used multiple pulses to manipulate electron-transfer processes;[18] Shen has separated ground-state and excited-state reorientation times;[19] and a number of people have used multiple excitations to identify intermediate states in electronic relaxation.[20−29]

More relevant to the current work are papers that have recognized that multiple-pulse experiments can distinguish between relaxation mechanisms that we would call homogeneous or heterogeneous. A multiple-pulse photolysis experiment was introduced by Fraunfelder[30] and elaborated by several others[31−34] to look at the nonexponential ligand rebinding in myoglobin. These experiments anticipate a number of key concepts in MUPPETS. They differ in relying on complete photolysis in at least two and up to 100 pulses. MUPPETS is a perturbative technique, which allows it to adopt the theoretical and experimental techniques from modern nonlinear spectroscopy and to generalize to a wide range of systems.

More recent multiple-pulse experiments are more similar to MUPPETS in design: Gaab and Bardeen developed a two-excitation anisotropy experiment to look at anomalous energy transport;[35,36] Larsen et al. used "pump-dump-probe" spectroscopy to discriminate between a homogeneous and an "inhomogeneous" model of the electronic-relaxation pathway in the photoactive yellow protein.[26] In those papers, the utility of multiple-pulse experiments was demonstrated for specific systems and specific relaxation processes. The current MUPPETS work is characterized by an emphasis on developing general methods, both theoretical and experimental, for separating homogeneous and heterogeneous relaxation mechanisms.

In our first paper, we not only defined the concepts of the MUPPETS experiment, but also applied it to two systems intended to demonstrate the effects of purely homogeneous and heterogeneous relaxation.[3,10] The process studied was ground-state recovery following electronic excitation of dye molecules. Auramine (Chart 1) is a dye that has a rapid and nonexponential excited-state decay. Glasbeek and co-workers have attributed this decay to a homogeneous mechanism: the phenyl groups twist in the excited-state and cause the relaxation rate to increase with time after excitation.[37−39] To form a sample with heterogeneous dynamics, the fast relaxing (∼15 ps) auramine was mixed with coumarin 102 (Chart 1), a dye molecule with a long (4.7 ns) relaxation time.

Each of these systems has a nonexponential decay, but they behave in a qualitatively different manner in a MUPPETS experiment (Figure 1). In a system where the nonexponential decay is solely due to heterogeneity, the MUPPETS signal measured for different values of the first delay time τ_1 should overlap onto a single curve if they are plotted as a function of the sum of the first and the second delay times, $\tau_1 + \tau_2$. Such plots are shown in Figure 1 for the MUPPETS data from the two systems just described. As expected, the MUPPETS data show that the nonexponential decay in the dye mixture is primarily due to heterogeneity, whereas the decay of nonexponential decay in auramine is not.

The purpose of this paper is to go beyond these qualitative conclusions and develop methods for the quantitative analysis of MUPPETS experiments, using the data shown above as examples. Two significant issues arise. The auramine decay is primarily homogeneous but also shows some evidence of heterogeneity. Thus, we are faced with a heterogeneous sample in which each component decay is itself nonexponential. It may be surprising, but we find that we do not need to assume a model for the form of the component decays; they can be derived uniquely from the MUPPETS data alone. We will present a quantitative fit to the data in Figure 1A based on two components and find the decay rates and decay forms for each component.

The second issue is the role of molecular rotation. It is well known that a polarized pump−probe experiment has two decay components: one due to electronic relaxation and one due to molecular rotation. In auramine, the electronic relaxation is faster than the rotation, so rotation has relatively little observable effect. However, the analysis of the mixture including coumarin requires a quantitative treatment of rotation in MUPPETS. Using this theory and the results from the pure auramine, the MUPPETS results in the auramine:coumarin mixture can be fit quantitatively as well.

Muppets Theory

Nonexponential Relaxation in Terms of Rate Correlation Functions. Our earlier paper presented the basic theory of the MUPPETS experiment.[3] Here, we review and expand on that presentation. The formalism deliberately mirrors the approach used in multidimensional coherence spectroscopies.[40] However, we will not emphasize that analogy here; it will be explored in more detail in an upcoming paper.[41]

We are concerned with a time dependent population $P(t)$, or more specifically, its deviation from its equilibrium value, $\delta P = P(t) - P_{eq}$. The population can be regarded as the occupation of a specific state; for current purposes, it can be the ground electronic state. However, these ideas generalize to any quantity that represents a quantum mechanical population (as opposed to a coherence).

The population relaxation is represented by a time dependent rate

$$k(t) = \frac{-1}{\delta P(t)} \frac{\mathrm{d}\delta P}{\mathrm{d}t} \tag{1}$$

In the case of an exponential decay, k is constant in time and is the standard rate constant. With a nonexponential decay, $k(t)$ varies with time. The time dependent rate is an alternative to describing a nonexponential decay as a sum of exponentials with different rates and amplitudes. In a heterogeneous sample, there may be subensembles, each of which has an exponential rate constant κ_i. The ensemble averaged rate will have a time

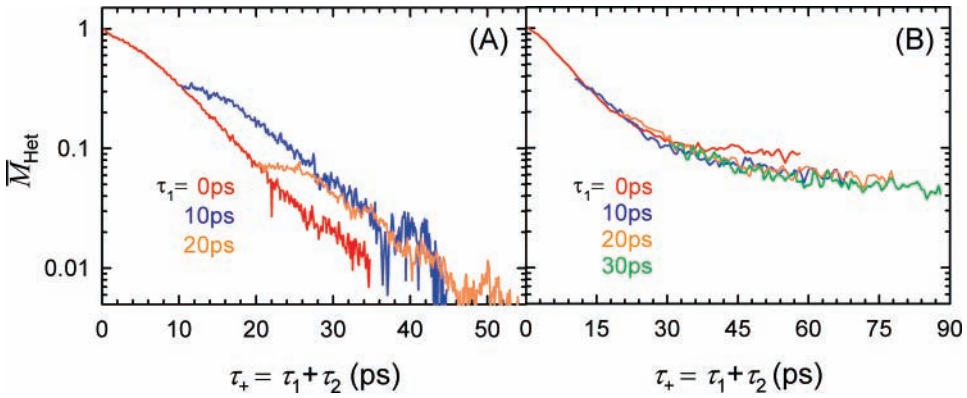

Figure 1. Log of the MUPPETS signals plotted against the sum of the two time periods for (A) pure auramine and (B) a mixture of auramine and coumarin, each in methanol.[3] Both systems show a nonexponential ground-state recovery. Curves for different values of τ_1 do not overlap in the case of homogeneous dynamics (A), but do overlap in the case of a purely heterogeneous dynamics (B).

dependent rate as defined by eq 1. However, the time-dependent rate also describes other situations, for example, the exchange of molecules between subensembles or cases where the time-dependence is homogeneous.

The population is perturbed from its equilibrium value by pulses of light in a manner that is described by a differential transition operator

$$\mathrm{d}T_j(t) = -\sigma_g E^*_{j'}(t) E_{j''}(t) \exp(i(\mathbf{k}_{j'} - \mathbf{k}_{j''})\cdot\mathbf{r}) + c.c. \quad (2)$$

where $E_j(t)$ represents the electric field of pulse j, $\mathbf{k}_j$ is the corresponding k-vector, $\mathbf{r}$ is the spatial position within the sample, and σ_g is the absorption cross section from the ground state to the excited state. This formula neglects the spatial envelope of the pulses to focus on the grating structure. Changing a population requires two interactions with the electric field: the primed and double primed fields in eq 2. This equation allows for the case where the interactions come from two beams with different k-vectors. In this case, a population grating is created.[42−44] The negative sign indicates that we are calculating the ground-state bleach, although it is equally possible to consider the excited-state population instead.

Once created, the ground-state bleach decays from time t_1 to t_2, as described by the time-evolution operator $G(t_2, t_1)$. Solving eq 1 gives

$$G(t_2, t_1) = \exp(-\int_{t_1}^{t_2} k(t)\mathrm{d}t) \quad (3)$$

In the last stage of the experiment, the population is measured. A probe field E_{pr} scatters from the population grating and is mixed with a local oscillator E_{LO} to create a heterodyned signal

$$S = (\sigma_g - \sigma_e) \int \mathrm{d}t\, \mathrm{d}\mathbf{r}\, E^*_{LO}(t) E_{pr}(t) \exp(i(\mathbf{k}_{LO} - \mathbf{k}_{pr})\cdot\mathbf{r}) \times \langle \delta P(t) \rangle + c.c. \quad (4)$$

The pointed brackets indicate that the signal is an ensemble average over the entire sample. It is assumed that the phase of the local oscillator is set to detect changes in absorption, not in index-of-refraction. The cross section for excited-state absorption is σ_e. Note that excited-state absorption interferes with the detection step, but not with the excitation (eq 2). This equation also describes the simple case of detecting changes in the transmission of a single beam; in that case, $\mathbf{k}_{LO}$ and $\mathbf{k}_{pr}$ are identical.

In principle, stimulated emission from the excited-state could also be included in both the excitation and detection steps. For simplicity, we assume that the Stokes shift is large enough and fast enough that this contribution can be neglected. This case holds reasonably well for the systems examined here.

In addition to its ability to boost signal size and reject undesirable signals, heterodyne detection is desirable because it creates a signal that is linear in the population. The signal in a homodyne experiment is proportional to the square of $\delta P(t)$. If the population decay is nonexponential and contains different decay components, the square of the decay will also contain cross terms between each pair of decay components. Thus, determining the shape of a nonexponential decay is easier with heterodyne detection.

In a standard, one-dimensional relaxation experiment, there is a single excitation and a single evolution period; to first order in perturbation theory, the final population is

$$\delta P^{(1)}(t_1, t_2; r) = G(t_2, t_1)\mathrm{d}T_1(t_1) P_{eq} \quad (5)$$

If the excitation and probe are separated by a time τ, the signal is

$$S(\tau) = (\sigma_g - \sigma_e)\sigma_g \int \mathrm{d}t_2\, \mathrm{d}t_1 E^*_{2''}(t_2 - \tau) E_{2'}(t_2 - \tau) E^*_{1''}(t_1) \times E_{1'}(t_1) \langle G(t_2, t_1) \rangle + c.c. \quad (6)$$

where we take $P_{eq} = 1$. The probe and local oscillator are simply described as the second pulse pair 2′ and 2″, respectively. The spatial integral has been done and yields the phase matching condition

$$\mathbf{k}_{2''} = \mathbf{k}_{2'} \pm (\mathbf{k}_{1''} - \mathbf{k}_{1'}) \quad (7)$$

Specializing to delta-function light pulses and defining the integrated "intensity" of a pulse pair as

$$I_j = \int \mathrm{d}t\, E^*_{j''}(t) E_{j'}(t) \quad (8)$$

yields a final expression for a one-dimensional kinetics experiment

$$S(\tau) = I_2 I_1 (\sigma_g - \sigma_e)\sigma_g \langle \exp(\int_0^\tau k(t')\mathrm{d}t') \rangle \quad (9)$$

This expression applies equally well to the change in transmission measured in a two-beam pump−probe experiment or in a four-beam, heterodyne detected transient grating.[45,46] A nonexponential signal can arise either from a rate constant $k(t)$ that is inherently time-dependent before ensemble averaging (homogeneous relaxation) or from an ensemble average over different rates (heterogeneous relaxation).

The approach just used can be easily extended to two excitations and two evolution periods. In this case, the final population is

$$\delta P^{(2)}(t_1, t_2, t_3; r) = G(t_3, t_2)\mathrm{d}T_2(t_2)G(t_2, t_1)\mathrm{d}T_1(t_1)P_{\mathrm{eq}} \quad (10)$$

The corresponding phase-matching condition is

$$\mathbf{k}_{3''} = \mathbf{k}_{3'} \pm (\mathbf{k}_{2''} - \mathbf{k}_{2'}) \pm (\mathbf{k}_{1''} - \mathbf{k}_{1'}) \quad (11)$$

Assuming delta-function light pulses with time τ_1 between the excitations and time τ_2 between the second excitation and probe, the MUPPETS signal is

$$M(\tau_1, \tau_2) = I_3 I_2 I_1 (\sigma_g - \sigma_e)\sigma_g^2 \langle \exp(-\int_{\tau_1}^{\tau_1+\tau_2} k(t'')\mathrm{d}t'' - \int_0^{\tau_1} k(t')\mathrm{d}t') \rangle \quad (12)$$

The key result is that the MUPPETS experiment measures the relaxation of each molecule twice over periods τ_1 and τ_2 before ensemble averaging. As a result, MUPPETS can distinguish between nonexponentiality due to ensemble averaging from nonexponentiality inherent in each subensemble.

The integral over t' in eq 12 represents the excitation and relaxation of a molecule during τ_1; the integral over t'' represents a second excitation and relaxation during τ_2. If a molecule has an inherently time dependent relaxation rate, this time dependence will be exactly the same in the first and second relaxation: these two relaxations are uncorrelated. On the other hand, a specific molecule in a heterogeneous sample may have a rate k_i that is greater or lesser than the average. This difference from the average persists over both excitation-relaxation cycles; the two integrals in eq 12 are correlated. Thus, homogeneous and heterogeneous sources of nonexponentiality correspond to uncorrelated or correlated rates in two relaxation periods. A one-dimensional relaxation measurement can only measure the ensemble averaged decay. The two-dimensional MUPPETS experiment is needed to measure correlations in this rate over time.

Before considering the implication of this result in more detail in the next subsection, a few comments on the signal amplitude are in order. We have assumed that excited-state absorption is followed by very rapid relaxation from the higher excited-state to the first excited-state and has no other effect on the kinetics. As a result, excited-state absorption only reduces the size of the signal and does so to an equal extent in either a one-dimensional or two-dimensional experiment. When trying to disentangle heterogeneity using spectral differences between components, excited-state absorption create more substantial complications, especially if the excited-state absorption spectrum evolves after excitation.

MUPPETS is a six-wave mixing experiment, so the size of the signal is a concern. Comparing eqs 9 and 12, the ratio of signal size in a MUPPETS experiment to that in a corresponding pump−probe experiment is $I\sigma_g$. For weak excitation, this is a factor equal to the fraction of molecules excited by a single pulse pair. It is common to excite 1−10% of the molecules in a pump−probe experiment, so the MUPPETS signal will be reduced from the pump−probe signal by a factor of 10−100. On allowed transitions, pump−probe signals are easily detected, so MUPPETS should have a broad range of applicability.

MUPPETS Experiment Is Related to One-Dimensional Experiments in Limiting Cases. For the remainder of the discussion, we will neglect the factors that only affect the signal size and focus on the decay behavior of the MUPPETS and pump−probe experiment. The signals will be normalized at the origin, $S(0) = 1$ and $M(0,0) = 1$. These two experiments are related in a simple way in certain limiting cases. First we note that if either of the time periods is set to zero, the MUPPETS experiment is identical to a one-dimensional experiment without any further approximations

$$M(0, \tau_2) = S(\tau_2) \quad (13)$$

and

$$M(\tau_1, 0) = S(\tau_1) \quad (14)$$

We can precisely define a homogeneous relaxation as one in which the decay during the first period is uncorrelated with the decay during the second period. A good example is given by auramine. Auramine is planar in the ground-state and twists to a nonplanar conformation in the excited state. The decay rate is a function of the twist angle, so the decay rate is truly a function of time after excitation. However, once a molecule relaxes, it returns to the planar ground state and undergoes exactly the same sequence of events after a second excitation. This statement is true whether the first relaxation happened to occur immediately after the excitation or long after the excitation.

In this case of uncorrelated or purely homogeneous relaxation, the two-dimensional MUPPETS experiment reduces to the product of one-dimensional experiments

$$M(\tau_1, \tau_2) = \langle \exp(\int_0^{\tau_2} k(t'')\mathrm{d}t'') \rangle \langle \exp(\int_0^{\tau_1} k(t')\mathrm{d}t') \rangle = S(\tau_1)S(\tau_2) \quad (15)$$

If the MUPPETS data is considered as a set of decays in τ_2 with different values of τ_1, and if each decay is normalized at $\tau_2 = 0$, then

$$\bar{M}(\tau_2; \tau_1) = \frac{M(\tau_2, \tau_1)}{M(0, \tau_1)} = S(\tau_2) \quad (16)$$

where the bar indicates a renormalized decay. The MUPPETS decay in τ_2 is the same as the decay in a one-dimensional experiment and is invariant to the value of τ_1.

The second limiting case is when the nonexponential decay is solely due to the presence of dynamic heterogeneity. In this case, the rate is a constant for each subensemble. Furthermore, that constant is perfectly correlated between the two time periods of the MUPPETS experiment; if a molecule relaxes rapidly after the first excitation, it will also relax rapidly after the second excitation. The heterogeneity need not be permanent: molecules can exchange between subensembles, so long as the exchange time is significantly longer than the total range of the MUPPETS experiment.

This limit leads to

$$M(\tau_1, \tau_2) = \langle \exp(-\kappa_i(\tau_1 + \tau_2)) \rangle_i = S(\tau_1 + \tau_2) \quad (17)$$

Because this limit arises from a heterogeneous distribution of exponential decays, we will denote this as the heterogeneous-exponential case.

The heterogeneous and homogeneous cases become degenerate, if and only if, the one-dimensional decay $S(t)$ is a single exponential. In this case, $S(\tau_1)S(\tau_2) = S(\tau_1 + \tau_2)$. The ideas of homogeneous and heterogeneous relaxation play no role when

the one-dimensional relaxation is exponential, and the MUPPETS experiment is not useful in this case.

A set of MUPPETS decays in τ_2 for specific values of τ_1 can be plotted to test for the heterogeneous limit in the following way. A time axis of $\tau_+ = \tau_1 + \tau_2$ is used so that each decay is shifted horizontally by an amount τ_1. The signals are normalized vertically so that the first point matches the $\tau_1 = 0$ decay

$$\bar{M}_{\text{het}}(\tau_+; \tau_1) = \frac{M(0, \tau_1)}{M(\tau_1, 0)} M(\tau_1, \tau_+ - \tau_1) = S(\tau_+) \quad (18)$$

If the heterogeneous-exponential limit holds, the curves for different values of τ_1 should overlap onto a single curve. Examples of these plots are shown in Figure 1. In Figure 1B, the curves overlap, showing that the nonexponential decay (from the dye mixture) is primarily heterogeneous. On the left-hand side, the curves overlap very poorly, showing that this nonexponential decay (from pure auramine) is not primarily due to heterogeneity.

A more detailed examination of the auramine data (see below) shows that it does not fit the purely homogeneous limit (eq 16) either. We are led to consider a limit in which there are subensembles that exchange slowly, but in which each subensemble may have a homogeneously nonexponential decay. We call this the heterogeneous−homogeneous limit, and it results in the following signal for a one-dimensional experiment

$$S(\tau) = \sum_i a_i S_i(\tau) \quad (19)$$

and the following MUPPETS signal

$$M(\tau_1, \tau_2) = \sum_i a_i S_i(\tau_2) S_i(\tau_1) \quad (20)$$

with $\sum_i a_i = 1$. The implications of this formula are more easily seen if the MUPPETS signal is normalized as in eq 16

$$\bar{M}(\tau_2; \tau_1) = \sum_i A_i(\tau_1) S_i(\tau_2)$$

$$A_i(\tau_1) = a_i \frac{S_i(\tau_1)}{S(\tau_1)} \quad (21)$$

with $\sum_i A_i = 1$. The MUPPETS decays in τ_2 are a superposition of the decays of each subensemble, but the contribution of each subensemble is dependent on the value of τ_1. The relative contribution of a subensemble decreases as τ_1 increases if the subensemble decay $S_i(\tau)$ is faster than the ensemble averaged decay $S(\tau)$. On the other hand, the relative contribution of a subensemble increases as τ_1 increases if the subensemble decay $S_i(\tau)$ is slower than the ensemble averaged decay $S(\tau)$. Thus the first time period of this MUPPETS experiment acts as a dynamic filter to remove rapidly decaying molecules. The decay of this filtered set of molecules is measured during τ_2.

The heterogeneous−homogeneous model is an approximation. It assumes that the time dependent rate is either fully correlated or completely uncorrelated between the two time periods of the MUPPETS experiment. For example, if molecules exchanged between dynamical subensembles on a time scale similar to the decay rates within each subensemble, the heterogeneous−homogeneous model would fail. This model can be compared to the inhomogeneous−homogeneous model of line shapes. In that model, the frequency correlation time is either much faster than or much slower than the phase decay. As a result, the line shape can be described as an inhomogeneous distribution of homogeneously broadened lines. That model fails when spectral diffusion is fast enough to cause partial motional narrowing. This analogy will be developed in detail in a future publication.[41]

Optical Design

MUPPETS is a $\chi^{(5)}$ nonlinear process using five excitation fields to produce the signal. Unlike many $\chi^{(5)}$ experiments, all interactions are resonant with a strong transition. As a result, neither absolute signal size nor cascaded processes are major problems. The experimental design is driven by the need to reject potentially stronger $\chi^{(3)}$ processes.

In principle, the MUPPETS experiment could be done with each pair of interactions (1′/1″, 2′/2″ and 3′/3″) coming from a single beam. The phase-matching in such a three-beam configuration provides no discrimination against $\chi^{(3)}$ processes. Careful subtraction routines to isolate the desired signal are needed in this case.[24]

By using a six-beam configuration and more complex phase-matching conditions, we isolated the desired $\chi^{(5)}$ MUPPETS signal from other competing processes. The resulting six-beam MUPPETS experiment can be viewed as a high-order extension of the heterodyne detected transient-grating experiment.[45,46] We have adopted a diffractive-optics approach to provide passive phase stabilization.[45−55] Our extension of this approach from four to six beams required the resolution of three major problems: design of a phase-matching pattern, correction of spherical aberration and elimination of single-beam bleaching effects. A schematic of the final optical setup is shown in Figure 2.

The phase-matching pattern chosen is shown in Figure 2. Each excitation wavevector ($\mathbf{k}_{1'}$-$\mathbf{k}_{1''}$ and $\mathbf{k}_{2'}$-$\mathbf{k}_{2''}$) is only half the length of the detection wavevector ($\mathbf{k}_{3''}$-$\mathbf{k}_{3'}$). Thus detection of processes involving only a single excitation are not phase matched. The symmetry pattern−reflection symmetry about the diagonals, but not about the vertical and horizontal axes−is important. It creates good phase matching for processes combining a 1 and 2 excitation, but poor phase-matching for double interactions of 1 and 1 or 2 and 2. The principles of the design process will be discussed in a future publication.

The phase-matching pattern is also designed so it can be generated from two standard transmission gratings (G1 and G2, INO optics), rather than a custom designed diffractive optic. The first grating (G1) serves primarily as a beam splitting mechanism. The region before G2 is not phase sensitive. Placing the delay lines between gratings G1 and G2 means that they do not need to be phase-stable delays. It also makes simultaneous scanning of the pulse pairs easy.

The silica gratings are identical with 96 g/mm, producing a full angle of 4.4° between the ±1 diffraction orders. The groove shape and depth are optimized to yield three equal intensity beams corresponding to 0 and ±1 diffraction orders. Approximately 10% is lost to higher orders. The L1−G1 distance is slightly less than the L1 focal length (fl) of 200 mm. Grating G1 is imaged onto the sample, so moving L1 adjusts the size of the beam both on G1 and at the final crossing point in the sample.

Lenses L2 (175 mm fl) and L3 (150 mm fl) image G1 onto G2. The grooves of G2 are oriented at 90° relative to those of G1, yielding a pattern of nine beams. This pattern is masked (M1) to give the final six-beam phase-matching pattern. The

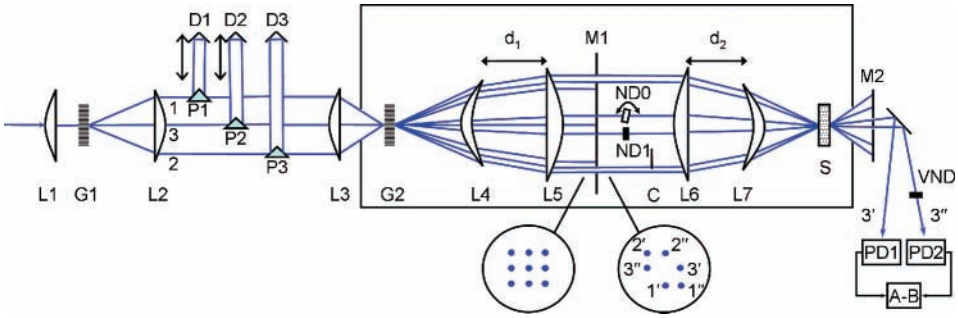

Figure 2. Schematic of the optical setup used in the MUPPETS experiments. Phase-stability is required in the region indicated by the box. The beam patterns are shown in the inset circles. L1−7, lenses; G1 and G2, gratings with grooves oriented in perpendicular directions; P1−3, reflective prisms that can be moved in and out of the beams to engage delay lines D1−3; M1−2, masks; C, chopper; ND0−1, neutral density filters; VND, variable neutral density filter; S, sample; PD1−2, matched photodiodes; and A-B, difference inputs of a lock-in amplifier.

pattern is slightly rectangular, because L2 and L3 are not identical, but this feature is not important. Each time-coincident pair of pulses in the final pattern is derived from a single beam coming from grating G1 and can be scanned by a single delay line. Delay lines D1 and D2 were varied to produce the times τ_1 and τ_2, respectively. Reflective prisms P1−P3 could be removed for initial alignment of the experiment and then reinserted to introduce time delays.

The beam pattern emerging from G2 must be reimaged onto the sample. An often unstated issue in using diffractive optics is that the imaging system between the optic and the sample must have near diffraction limited performance not just over the diameter of one beam but over the entire aperture covered by the beam pattern. Reflective paraboloids are popular in diffractive-optics schemes because of their low chromatic dispersion and negligible spherical aberration. However, paraboloids have high coma, distort out-of-plane polarizations, and produce cramped set-ups due to the need for folded geometries and small apertures.

We have chosen to use lenses to avoid these problems. Lenses L5 and L6 have 4 in. diameters and 500 mm focal lengths. As a result, the beam separations are large in the region between these lenses (e.g., 25 mm from 1′ to 1″). These large separations give flexibility in adding optics in this region to manipulate each of the six beams individually.

With singlet lenses, spherical aberration is the dominant aberration and is problematic, even with long focal length lenses. In the four-beam transient grating experiment, a square pattern with each beam equidistant from the centers of the lenses is normally chosen. Each beam experiences exactly the same spherical aberration, so no correction for this aberration is needed in the four-beam experiment. However, in the six-beam MUPPETS experiment, spherical aberration is unavoidable. A beam pattern sufficiently symmetric to avoid spherical aberration will not discriminate against all $\chi^{(3)}$ processes.

To deal with the problem of spherical aberration, we have introduced two meniscus lenses (L4 and L7) approximately half way between the collimating lenses and their foci. These lenses create a negative spherical aberration to compensate the normal aberrations in the other lenses. Small movements of these lenses along the beam direction (d_1 and d_2) vary the total aberration of the system continuously. The beam pattern at the sample is magnified onto an inexpensive camera to provide a direct diagnostic for this adjustment.

Another issue with lenses is that the group delay for different beams is not identical. When the aberrations are corrected, the phase delay between the object at G2 and the image at S is guaranteed to be identical for all the beams. However, beams passing through the lenses at different radial distances pass through different amounts of glass and have different group delays. Thus, pulses pairs 1′−1″ and 2′−2″ do not have identical arrival times. Thin silica plates (ESCO Products) were introduced between L5 and L6 to correct for the delay differences.

Phase stability is only required within the pairs of excitation and detection beams but is not needed between pulse pairs. As a result, only the area between G2 and the sample S needs to be phase-stable. The entire setup is on a vibration isolated table with laminar air flow, and the region between G2 and S is enclosed to exclude air currents. No active phase stabilization is used.

A disadvantage of the diffractive-optics approach to heterodyne detection is that the strength of the local oscillator is altered by the bleaching of the sample by each, individual excitation beam. A chopper placed in beam 1′ combined with lock-in detection eliminates the single-beam bleaching effects due to all beams except 1′. Solutions have been proposed to deal with this remaining artifact: a separate optical stage to generate the local oscillator[49] or displacing the local oscillator at the sample and re-establishing overlap with the signal at the detector.

We have devised a relatively simple solution based on balanced detection of the probe (3′) and local oscillator (3″) beams. Each beam is detected on a matched photodiode (PD1 and PD2) and the signals are subtracted using the difference inputs of the lock-in amplifier. A variable neutral density filter (VND) is used to zero the signal in the absence of a MUPPETS signal (e.g., $\tau_2 < \tau_1 = 0$). Any bleaching of the sample affects both beams equally and cancels in the difference measurement.

Ogilvie et al. have shown that if the intensities of the probe and local oscillator are exactly matched at the sample, then only the refractive portion of the final grating contributes to the signal.[47] In a future publication, we will discuss the converse case: if the probe is much weaker than the local oscillator at the sample, then only the absorptive component of the grating is detected.[56] We use this method in the current experiments.

The condition for detecting absorptive signals was created by putting a neutral density filter (ND1) in beam 3′ before the sample. The variable neutral density filter VND rebalanced the intensities of 3′ and 3″ at the detectors. A similar blank glass plate (ND0) in beam 3″ matched the travel time of 3′ and 3″. This plate was also rotated to vary the phase of the local oscillator.

Experimental Details

The pulse entering the experiment was the frequency doubled output (398 nm) of a 1 kHz amplified Ti:sapphire laser with a pulse width of 40 fs. Dispersion in the optics led to a pulse width of approximately 200 fs at the sample. Because this width

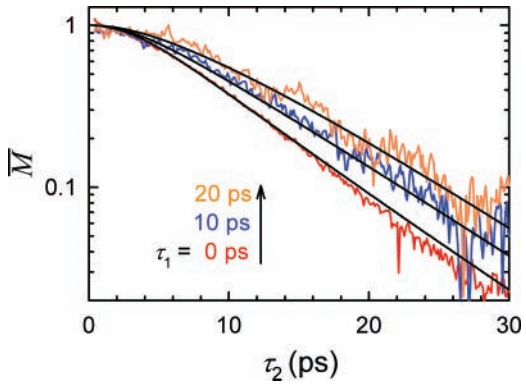

Figure 3. MUPPETS data on pure auramine in methanol normalized according to eq 16. The curves should overlap if the nonexponential decay is purely homogeneous. The solid curves are fits to a model with two components, each with a homogeneous nonexponential decay (eqs 22 and 31). See Figure 6 for parameters.

is much smaller than the measured decay times, no effort was made to compensate the dispersion.

The input pulse had energy of 2.5 μJ. Higher energies produced spectral broadening as the pulse passed through grating G1. At the sample, each excitation beam and the local oscillator had energies of 0.25 μJ. The energy of the probe beam (3′) was ten times lower at the sample. The beams had 200 μm diameters at the sample.

The samples were contained in a 1 mm path length silica cuvette. Both samples consisted of methanol solutions with the concentrations adjusted to produce an absorbance of 0.5 at 400 nm: 0.4 mM in the pure auramine sample and 0.17 mM auramine plus 0.14 mM coumarin 102 in the mixed sample. With the beam intensity used, the bleaching by a single excitation beam in the auramine sample was 2%.

The photodiodes PDA and PDB were used in photoconductive mode with a common voltage source. The photodiodes were unamplified and had carefully matched RC time constants. The signals from the detectors were subtracted using the difference inputs of the lock-in amplifier. A synchronized chopper blocks every other pulse in beam 1′. Scans of the lock-in signal were collected with ND0 rotated to produce the maximum signal and the minimum signal. Subtraction of these two scans produced the final result.

Pure Auramine and the Decomposition of MUPPETS Data into Subensemble Decays

Qualitative Assessment of the Auramine Results. MUPPETS data from the pure auramine solution are shown on the left of Figure 1. The decays are clearly nonexponential with a slow initial rate evolving into a more rapid exponential tail at long times. This plot is designed to detect pure heterogeneous broadening (eq 18), and it shows that auramine's nonexponentiality is not primarily due to sample heterogeneity. This result is entirely expected from the proposed mechanism in which the electronic relaxation rate increases as the molecules twists in the excited state.

This mechanism predicts that the nonexponentiality is purely homogeneous. In that case, the three curves should overlap perfectly in the plot shown in Figure 3 (eq 16), and they do not. Using the idea that increasing τ_1 filters out the effect of rapidly decaying molecules, it appears that the sample has some degree of dynamic heterogeneity. The decay slows as τ_1 increases. However, even when $\tau_1 = 20$ ps, nonexponentiality remains for $\tau_2 < 10$ ps. Thus, each dynamic subensemble must have a homogeneous nonexponential decay. The simplest model consistent with the data is a two-component (fast f and slow s) heterogeneous−homogeneous model

$$M(\tau_1, \tau_2) = a_f S_f(\tau_1) S_f(\tau_2) + a_s S_s(\tau_1) S_s(\tau_2) \qquad (22)$$

with $a_f + a_s = 1$.

Moving beyond this qualitative assessment and developing a quantitative interpretation of the data presents a challenge. Two functions of undetermined form, S_f and S_s, are needed to fit the data. The proposed mechanism provides little guidance: the form of the torsional potential and the dependence of the rate on torsional angle are not well understood and not easily reduced to a fitting function.

One could guess at empirical model functions for S_f and S_s and hope to find an adequate fit. However, there is no guarantee that this strategy will work. Moreover, even after finding one fit, one does not know how much flexibility there is in the result. For example, assume that a fit is found in which S_f and S_s have different shapes. Is this difference a requirement of the data, or could they have similar shapes if a different model function were assumed?

This section of the paper demonstrates a different approach. MUPPETS data can be used to derive experimental decays for S_f and S_s without a priori assumptions on the forms of these decays. Being experimental results, these decays retain noise. One can legitimately ask questions such as the following: do S_f and S_s differ in shape by more than the experimental error?

Model-Free Decomposition of MUPPETS Data. We assume that there are two dynamical subensembles (eq 22) and that we have collected MUPPETS curves along τ_2 for at least three values of τ_1: τ_1°, τ_1', and τ_1''. For convenience in the discussion, we take these times to be in the temporal order listed, although this order is not essential.

We begin by considering just the first two curves at τ_1° and τ_1'. The fast component should contribute more to the first decay, and the slow component more to the second decay. After normalizing the MUPPETS data according to eq 16, a trial result for S_f is obtained by subtracting a fraction f_1' of the later decay from the earlier one

$$S_f'(\tau_2) = \frac{\bar{M}(\tau_2; \tau_1^\circ) - f_1' \bar{M}(\tau_2; \tau_1')}{1 - f_1'} \qquad (23)$$

Similarly, a trial result for S_s is obtained by subtracting a fraction f_2' of the earlier decay from the later one

$$S_s'(\tau_2) = \frac{\bar{M}(\tau_2; \tau_1') - f_2' \bar{M}(\tau_2; \tau_1^\circ)}{1 - f_2'} \qquad (24)$$

The two parameters f_1' and f_2' are initially arbitrary. Certain basic physical constraints apply: S_f and S_s should not be negative and should decay, not rise with time. (This assumption is reasonable for the current system, but for other systems different constraints may be appropriate.) More importantly, the heterogeneous−homogeneous approximation (eq 22) implies a constraint on these two parameters and the functions derived by using them

$$f_2' \frac{S_s'(\tau')}{S_s'(\tau)} = \frac{1}{f_1'} \frac{S_f'(\tau')}{S_f'(\tau)} \qquad (25)$$

Thus, one obtains a one-dimensional range of self-consistent parameter pairs (f_1', f_2') and associated decay functions.

This procedure is repeated on a second pair of MUPPETS decays at τ_1° and τ_1''

$$S_f''(\tau_2) = \frac{\bar{M}(\tau_2; \tau_1^\circ) - f_1'' \bar{M}(\tau_2; \tau_1')}{1 - f_1''} \quad (26)$$

$$S_s''(\tau_2) = \frac{\bar{M}(\tau_2; \tau_1'') - f_2'' \bar{M}(\tau_2; \tau_1^\circ)}{1 - f_2''} \quad (27)$$

However, the parameters f_1'' and f_2'' are not arbitrary. They are fully determined by two conditions: the amplitudes a_s and a_f derived from each pair of times, τ_1°/τ_1' and τ_1°/τ_1'', must be the same, $a_s' = a_s''$ and $a_f' = a_f''$, and the values of the extracted components must be the same at τ°, $S_f'(\tau^\circ) = S_f''(\tau^\circ)$ and $S_s'(\tau^\circ) = S_s''(\tau^\circ)$. These conditions yield the following formulas:

$$f_1'' = f_1' + \frac{f_1' f_2' Q}{1 - f_1' f_2'}(1 - f_1') \quad (28)$$

$$f_1'' f_2'' = Q f_1' f_2' \quad (29)$$

$$Q = \frac{S_s'(\tau') S_f'(\tau'')}{S_s'(\tau'') S_f'(\tau')} \quad (30)$$

We now have a set of possible decompositions of the data that can be described by a single parameter, f_1; all other parameters are determined by self-consistency requirements (eqs 25 and 28−30). These equations guarantee that the component decays extracted from each pair of MUPPETS decays match at a single point in time; they do not guarantee that the component decays will match at every time. Requiring that the two determinations each yield the same decays allows one to uniquely determine the best decomposition of the data.

This procedure was used on the pure auramine data (Figure 3). Three possible solutions are shown in Figure 4. The component decays S_f and S_s determined from the $\tau_1 = 0$ and 10 ps data are shown in red; the decays determined from the $\tau_1 = 0$ and 20 ps data are shown in blue. If f_1 is too low (Figure 4A), S_s has a physically unrealistic rise at early times. If f_1 is too large (Figure 4C), $S_f(\tau)$ is not consistent between the two determinations. Thus, we are led to a single optimum value of $f_1 = 0.43 \pm 0.03$, and a unique decomposition of the MUPPETS data into two heterogeneous decay components. This value of f_1 implies that the relative amplitudes of the two components are $a_f = 0.75$ and $a_s = 0.25$.

This procedure does rely on the assumption that there are exactly two components. However, this assumption is disprovable. If there is only one component, the procedure will either yield $S_f(\tau) = S_s(\tau)$ or it will set the amplitude of one component to zero. If there are three sufficiently different components, no fully self-consistent solution will exist. Of course, if two of these three components are sufficiently similar in shape and decay time, they may not be resolvable within the experimental noise.

A common simplification in modeling nonexponential decays is that all the component decays have similar shapes. In other words, all decays can be superimposed onto a single master function by stretching or compressing the time scale, $S(\tau) = S_f(\tau/\tau_f) = S_s(\tau/\tau_s)$. This simplification has not been imposed in the decomposition of the MUPPETS data. Rather this idea can be tested from the experimental results.

This test is done on the auramine results in Figure 5. The two determinations of each decay function have been averaged, and then the time scales and relative amplitudes of the fast and slow decays have been scaled to match the two decays at long time. Nonetheless, the two curves differ at early times. This difference in shape is outside the scatter of the data. It is an experimental finding, not an artifact of the assumptions used in the fitting.

Quantitative Fitting of the Auramine Data. In the previous subsection, MUPPETS data were deliberately analyzed without selecting an analytical model function to describe the component decays. However, now that the analysis is complete, it is convenient to develop such a description. Inspection of Figures 4 and 5 show that the decays are exponential in the tail and relatively flat in the beginning. Moreover, the extent of the flat initial portion differs between the fast and slow components.

A model function based on the hyperbolic secant

$$S_i(\tau) = \mathrm{sech}^{\beta_i}\left(\frac{\tau}{\beta_i \tau_i}\right) \quad (31)$$

has proven sufficient to fit the component decays. At long times, this function approaches an exponential decay with a time constant of τ_i. The parameter β_i determines how far the slow region at the beginning of the decay lasts. Figure 6 shows fits to this function. From these fits, the limiting time constants are in a ratio of 0.6. As expected, the shapes of the decay differ: $\beta_f = 1.1$, but $\beta_s = 1.7$.

To double check the quality of these fits, the results can be compared to the original MUPPETS data using eq 22. The results are shown in Figure 3. There is no further adjustment of parameters at this point. The agreement with the data is good, as expected. A careful examination of the first 1.5 ps of the $\tau_1 = 0$ data shows a small and very rapid decay component that is not present in the other curves and does not fit the model. Because it is too small to characterize accurately, we have simply left this feature out of our fitting by only using times greater than 1.5 ps in analyzing the data.

The fits to the component decays can also be used to derive time dependent relaxation rates for each subensemble of auramine, as defined in eq 1. These curves are shown in Figure 7. The time dependent rates should be more closely related to the time dependent torsional angle in auramine; the rate should be a product of the angle and the angle dependent electronic coupling. The long time value of the rate should be the rate at the equilibrium torsional angle in the excited state.

These results give some information on the nature of the two subensembles. One can envision two ways that the torsional motion could be modified. In one case, the electronic structure of the auramine, that is, the shape of the torsional potential and the nonradiative rate as a function of torsional angle, are constant, but the torsional motion is slowed due to purely mechanical reasons. An example germane to auramine in methanol is solvent attachment by hydrogen bonding. Even without any changes in the torsional potential, the increased viscous drag would slow the torsional motion. A similar process is known to slow the rotation rate of some dye molecules in alcohols,[57,58] and auramine has several potential hydrogen-bond accepting sites.

If there were no differences in the electronic structure of the two subensembles, the internal conversion rates at long times should be the same; the subensembles would only differ in the time it takes to reach the long time rate. This case does not match the experimental results. Figure 7 shows that the final rates are substantially different. Either the minimum of the torsional potential is shifted to a larger angle in one of the subensembles, or the internal conversion rate at the minimum is increased in one of the subensembles.

Solvent attachment by hydrogen bonding does not typically cause strong changes in electronic structure as indicated by the data.[57] A mechanism more likely to cause strong perturbations

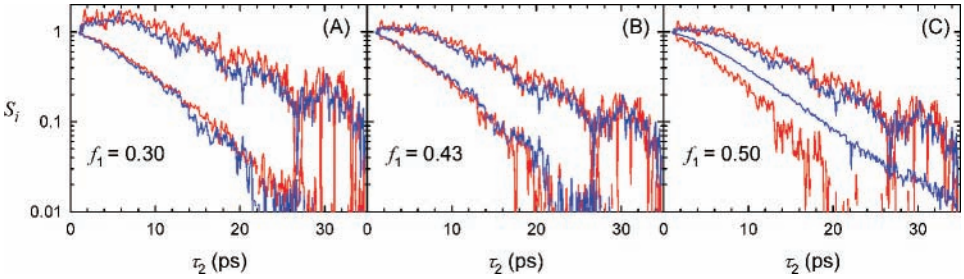

Figure 4. Individual decay components S_f (lower) and S_s (upper) extracted from the MUPPETS data on pure auramine (Figure 3) for different assumed values of f_1'. The red data is determined from the $\tau_1 = 0$ and 10 ps data; the blue data from the $\tau_1 = 0$ and 20 ps data. (B) is the correct fit. In (A), S_s initially rises instead of decaying; in (C), the two determinations of S_f do not agree.

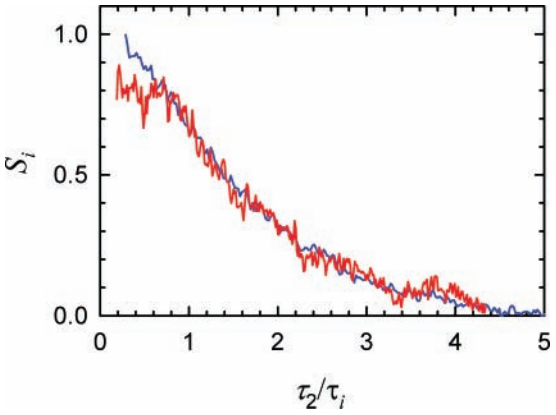

Figure 5. Comparison of the shapes of the fast (S_f, blue) and slow (S_s, red) components of the auramine decay. These decays have been scaled in amplitude and in time ($\tau_f = 4.9$ ps, $\tau_s = 8.0$ ps) to match the later parts of the decays. A difference in the shape of the early portions of the decays is evident.

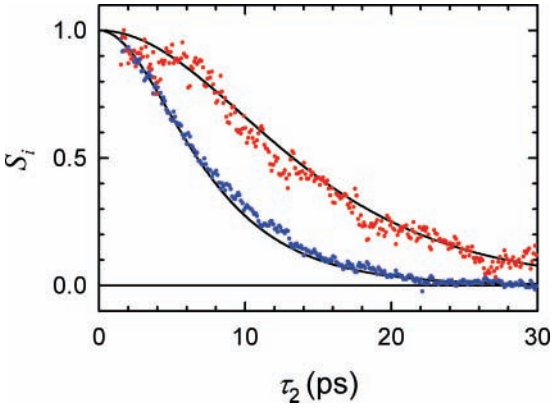

Figure 6. Fits to the fast and slow components of the auramine electronic-state relaxation. The points are averages of the two determinations of S_f (blue) and S_s (red) shown in Figure 4B. Fits to eq 31 are shown as solid curves: $\tau_f = 4.9$ ps, $\beta_f = 1.1$, $\tau_s = 8.0$ ps, $\beta_s = 1.7$.

is ion-pairing. Different resonance structures of auramine place the positive charge at different places in the molecule. An anion near the central nitrogen would greatly stabilize resonance structures with change on the central nitrogen (as shown in Chart 1) and thereby alter the overall electronic structure of the auramine.

No kinetic measurement by itself is definitive on the question of molecular structure. Further experiments are needed to settle the nature of the difference in the two kinetic subensembles. However, these arguments show that the existence of such subensembles is not only plausible but that they are expected to occur in at least some systems. MUPPETS can not only detect these subensembles, but can also determine important properties of them.

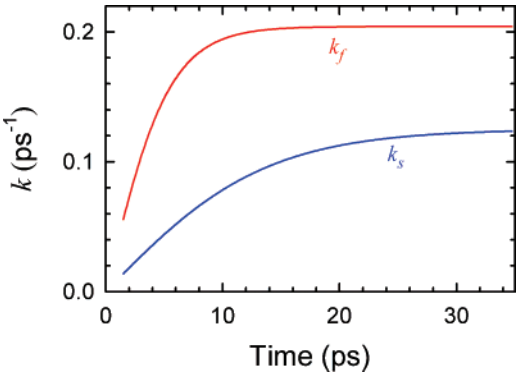

Figure 7. The time dependent electronic relaxation rates for the fast (red) and slow (blue) subensembles of auramine derived from the fits in Figure 6 and eq 1.

Auramine-Coumarin Mixture and the Effect of Rotation in MUPPETS

Qualitative Assessment of the Dye-Mixture Results. Coumarin and auramine have strongly overlapping absorption spectra, but whereas auramine has a nonexponential excited-state relaxation that is essentially complete within 30 ps, coumarin 102 in methanol has an exponential excited-state relaxation with a 4.7 ns time constant.[59] The mixture of the two should show a strong dynamic heterogeneity, and this expectation is confirmed in Figure 1B. With the parameters of the auramine decay derived in the last section and the known behavior of coumarin, it should be possible to quantitatively predict the MUPPETS data from the mixture.

There is one complication. The MUPPETS data on the mixture are replotted against τ_2 in Figure 8. The $\tau_1 = 0$ decay is strongly nonexponential because of the dynamic heterogeneity. As τ_1 increases, the contribution of the fast relaxing auramine is filtered out, and the long decay of the coumarin becomes more dominant. When $\tau_1 = 30$ ps, the auramine decay, which is essentially complete by this time, should be completely eliminated, but the data still show a rapid decay component.

However, rotation of the coumarin molecule is also expected to be on the tens-of-picosecond time scale. The next subsection discusses the role of rotation in MUPPETS in general. The following subsection shows that rotation accounts for the residual fast dynamics seen at $\tau_1 = 30$ ps in Figure 8.

Effect of Molecular Rotation in MUPPETS. In one-dimensional measurements of electronic-state populations, the signal is affected by rotation in a manner that depends on the relative polarization of the pump and probe excitations

$$S_{||}(\tau) = (1 + 2r(t))S(t) \tag{32}$$

$$S_{\perp}(\tau) = (1 - r(t))S(t) \tag{33}$$

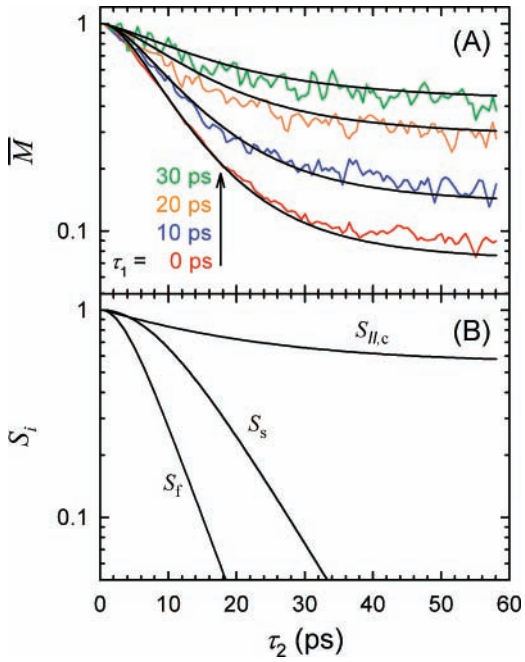

Figure 8. (A) MUPPETS data from a mixture of coumarin and auramine in methanol (noisy colored curves) and fits (smooth black curves). For small values of τ_1, the decay is a combination of the decays of both dyes. As τ_1 increases, the fast auramine decay is eliminated, leaving only the coumarin decay. The coumarin decay itself is biphasic, consisting of a fast rotation and a slow electronic relaxation. (B) The three component decays contributing to the mixture: the fast (S_f) and slow (S_s) auramine components and the coumarin component (S_c), as derived from the fits in (A).

where the signal is $S_{||}(t)$ in the case of parallel pump and probe polarizations, the signal is $S_{\perp}(t)$ in the case of perpendicular polarizations, and the signal is $S(t)$ in the rotationally averaged case. The rotational dynamics are governed by the anisotropy $r(t)$. Even in the absence of heterogeneity, the signal contains at least two decay components, corresponding to the orientation and population relaxations. (The anisotropy decay itself can be nonexponential, but a single exponential is often an adequate approximation.) In a MUPPETS experiment, does this two-phase decay behave homogeneously or heterogeneously?

If rotation is independent of the electronic dynamics, but each component of the system is allowed to have different rotational dynamics, then the MUPPETS signal with all polarizations parallel is

$$M_{||}(\tau_1, \tau_2) = \sum_i R_i(\tau_1, \tau_2) M_i(\tau_1, \tau_2) \tag{34}$$

where $M_i(\tau_1,\tau_2)$ is calculated without including rotation. Through a detailed calculation described in the Supporting Information, the rotational effect is found to be

$$R(\tau_2, \tau_1) = 1 + 2r(\tau_1) + 2r(\tau_2) + \frac{55}{7} r(\tau_1) r(\tau_2) \tag{35}$$

Combining the homogeneous−heterogeneous approximation (eq 20) with eqs 32−35 gives

$$M_{||}(\tau_2, \tau_1) = \sum_i a_i \left(S_{i,||}(\tau_2) S_{i,||}(\tau_1) + \frac{27}{7} r_i(\tau_2) S_i(\tau_2) \cdot r_i(\tau_1) S_i(\tau_1) \right) \tag{36}$$

in terms of the one-dimensional signals with parallel polarization $S_{i,||}$ and without rotational effects S_i.

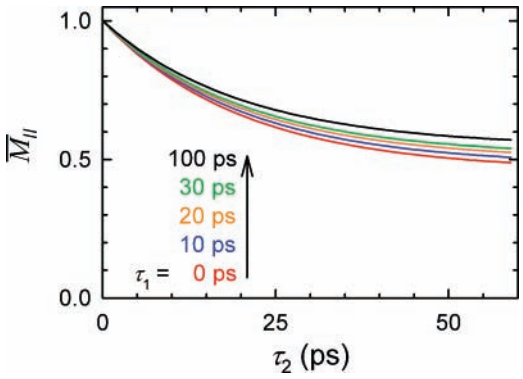

Figure 9. A model calculation of the effect of rotation in MUPPETS. The signal is calculated (eq 36) for a single component with an electronic relaxation time much longer than its rotational time (τ_r = 20 ps and τ_e = 4.7 ns). All polarizations are parallel. The nonexponential decay caused by rotation is only slightly affected by τ_1. The rotational-electronic decay nearly behaves like a single homogeneous process.

When the rotation is slower than the electronic relaxation, rotation has no effect on the MUPPETS signal. In this case, $S_{||}(t)$ approaches $S(t)$, $r(t)$ is approximately one, and eq 36 reduces to eq 20. This case applies to auramine. Rotation times of molecules similar to auramine are all greater than 85 ps in methanol,[60] which are times that are slower than its electronic relaxation. Thus, the neglect of rotation in analyzing the pure auramine results is justified.

The opposite limit is when the rotation is faster than the electronic relaxation. In this case, the effect of rotation is split into an apparently homogeneous part and an apparently heterogeneous part. In the second term of eq 36, the electronic relaxation can be neglected, $S(t) \approx 1$, leading to

$$M_{||}(\tau_2, \tau_1) \approx \sum_i a_i S_{i,||}(\tau_2) S_{i,||}(\tau_1) + \frac{27}{7} \sum_i a_i r_i(\tau_2) r_i(\tau_1) \tag{37}$$

In the first summation of eq 37, the decay due to rotation and due to electronic relaxation are not separated; $S_{||}(t)$ behaves as a homogeneous, nonexponential decay. In the second term, the rotational anisotropy behaves as like a separate heterogeneous contribution to the overall MUPPETS decay.

Although the nonexponential decay due to rotation has both homogeneous and heterogeneous properties, in practice the homogeneous properties dominate. This idea is illustrated in Figure 9, which shows calculations of individually normalized scans at fixed values of τ_1. In eq 36, a single component has been assumed with its rotational and electronic relaxations each taken to be a single exponential with time constants τ_r = 20 ps and τ_e = 4.7 ns respectively. (These values match the ones used for coumarin in the next subsection.) On the time scale in the figure, the electronic relaxation is essentially constant. The one-dimensional signal $S_{||}(t)$ for this system is a biexponential. The MUPPETS signal is also nonexponential. As τ_1 increases, the amplitude of the fast rotational component of the decay decreases slightly, reflecting a slight filtering of the rotational component, as if it were another component in the system. However, this effect is very slight. (Note the linear scale in Figure 9 compared to the log scale in most of the other figures.) To a good approximation, the MUPPETS experiment does not separate a fast rotation from a slow electronic decay of the same molecule.

Fitting MUPPETS Data from the Coumarin-Auramine Mixture. These ideas were used to understand the data taken in a mixture of coumarin and auramine in methanol. The data were fit as a mixture of three components: a fast and a slow auramine component, S_f and S_s, and a coumarin component with electronic decay S_c and anisotropy r_c. The auramine components were described by the fits to the pure auramine sample (Figure 6A). Rotation was included for the coumarin, but neglected for the auramine. Coumarin's rotational and electronic relaxation were each described by a single exponential. The electronic relaxation time of coumarin 102 is known to be 4.7 ns.[59] Only the coumarin rotation time and the ratio of the auramine and coumarin contributions to the signal needed to be adjusted.

The fits in Figure 8A are quite good. The rotation time of coumarin is 20 ps and the fraction of the signal due to coumarin is 4.5%. (Because the signal size is affected by both the ground-state and excited-state absorption cross sections, the relative signal size is not simply related to the relative concentrations.)

The success of the fits confirms that the rotational motion is being treated correctly. The components of the fits describing the three main contributions to the signal: S_f, S_s, and $S_{||,c}$; are shown in Figure 8B. As τ_1 increases, the auramine contributions are eliminated, leaving only the coumarin rotation-electronic decay at $\tau_1 = 30$ ps. At $\tau_1 = 30$ ps, a fast decay component remains due to the rotational motion of the coumarin.

Summary and Conclusions

This paper has looked at the analysis of MUPPETS data. Although the systems were chosen for demonstration purposes, they displayed a number of complicated features: short-lived dynamical subensembles, subensembles with only modestly different average rates, component decays that are nonexponential and have different shapes in different subensembles, decays that combine rotation, and electronic relaxation. Despite these complications, the MUPPETS experiment was able to extract the relaxation properties of each subensemble uniquely.

The difference between homogeneous and heterogeneous relaxation was related to time-correlations of a time-dependent rate. Whereas standard one-dimensional experiments measure the ensemble average of this time-dependent rate, a two-dimensional experiment such as MUPPETS is needed to measure its correlations. More specifically, we showed that the first time period in MUPPETS acts as a dynamical filter to remove fast relaxing molecules from a subsequent relaxation measurement in the second period.

To execute these two-dimensional, heterodyne detected experiments, a diffractive-optics setup was developed. The concept is based on diffractive-optics schemes for four-beam transient-grating experiments, but several innovations were needed for the six-beam MUPPETS experiment: continuously adjustable spherical aberration, balanced detection of the probe and local oscillator, and phase-matching patterns based on superimposing the images of multiple linear gratings.

The paper then looked at the quantitative analysis of the resulting MUPPETS data. In particular, we showed that it is not necessary to know the form of the decay within each subensemble. We did not assume that the subensembles have exponential decays nor even that they have similar decay shapes. Nonetheless, individual decays for each subensemble can be extracted from the MUPPETS data. This "model-free" analysis was demonstrated on the two auramine components. However, the method can be extended to any number of components, so long as their decay times differ sufficiently. In the auramine case, the ratio of decay times was 1.6, and the two components were easily separated. Even smaller ratios should be distinguishable.

Although the main focus of the paper was the development of the technical aspects of MUPPETS, new information on auramine emerged naturally from the data analysis. Before the MUPPETS experiment, it was not suspected that auramine was dynamically heterogeneous. In hindsight, there are plausible sources of transient heterogeneity, including solvent attachment or ion pairing. Van der Meer, Zhang, and Glasbeek previously found that the shape of the auramine decay is sensitive to the solvent, an observation that is consistent with a changing the ratio of the different dynamical species involved.[37] However, using only conventional experiments, it would be difficult to make a compelling case for dynamical heterogeneity.

Quantitative analysis of the MUPPETS data showed that two distinct subensembles were involved. These subensembles not only have different average electronic-relaxation times but also have different decay shapes. We suggested that ion-paired and nonpaired molecules are the origin of the two subensembles.

The last portion of the paper looked at the effect of MUPPETS on the two-phase, rotation/electronic relaxation typically seen in pump−probe measurements of solutes in liquids. To a very good approximation, the rotation and electronic relaxation decays of a single molecule are not separated in a parallel-polarization MUPPETS experiment. These predictions were confirmed by quantitative fits to MUPPETS data in a mixture of auramine and coumarin 102.

The current experiments can be straightforwardly extended in a number of directions. By using different frequencies for the different excitations and for the probe, MUPPETS can be applied to molecules with multiple states involved in the relaxation pathway. By combining the spectral resolution of different transitions with the dynamical resolution of MUPPETS, complex relaxation mechanisms can be unraveled. Alternatively, the different beams can be given different polarization. It should be possible to decompose dynamic heterogeneity in rotational motion as well as in electronic relaxation. Finally, additional time periods can be added to create three, or even higher, dimensional MUPPETS experiments. For example, experiments to measure the exchange time between different dynamical subensembles can be envisioned. The results of this paper help to lay the foundations for these future developments.

Acknowledgment. This work was supported by the National Science Foundation under Grant CHE-0210986.

Supporting Information Available: Derivation of eq 35. This information is available free of charge via the Internet at http://pubs.acs.org.

References and Notes

(1) *Disorder Effects On Relaxational Processes: Glasses, Polymers, Proteins*; Richert, R.; Blumen, A., Eds.; Springer: Berlin, 1994.

(2) Ediger, M. D. *Annu. Rev. Phys. Chem.* **2000**, *51*, 99.

(3) van Veldhoven, E.; Khurmi, C.; Zhang, X.; Berg, M. A. *ChemPhysChem* **2007**, *8*, 1761.

(4) Frauenfelder, H.; Wolynes, P. G. *Science* **1985**, *229*, 337.

(5) O'Neill, M. A.; Barton, J. K. *J. Am. Chem. Soc.* **2004**, *126*, 11471.

(6) Bouvier, B.; Dognon, J. P.; Lavery, R.; Markovitsi, D.; Millie, P.; Onidas, D.; Zakrzewska, K. J. *Phys. Chem. B* **2003**, *107*, 13512.

(7) Somoza, M. M.; Sluch, M. I.; Berg, M. A. *Macromolecules* **2003**, *118*, 2721.

(8) Barkai, E.; Jung, Y.; Silbey, R. *Annu. Rev. Phys. Chem.* **2004**, *55*, 457.

(9) Quitevis, E. L.; Marcus, A. H.; Fayer, M. D. *J. Phys. Chem.* **1993**, *97*, 5762.

(10) Khurmi, C.; van Veldhoven, E.; Zhang, X.; Berg, M. A. In *Ultrafast Phenomena XV*, Springer Series in Chemical Physics; Corkum, P., Jonas, D., Miller, R. J. D., Weiner, A. M., Eds.; Springer-Verlag: Berlin, 2007; Vol. 88, pp 329.
(11) Zanni, M. T.; Hochstrasser, R. M. *Curr. Opin. Struct. Biol*. **2001**, *11*, 516.
(12) Wright, J. C. *Int. Rev. Phys. Chem*. **2002**, *21*, 185.
(13) Jonas, D. M. *Annu. Rev. Phys. Chem*. **2003**, *54*, 425.
(14) Khalil, M.; Demirdoven, N.; Tokmakoff, A. *J. Phys. Chem. A* **2003**, *107*, 5258.
(15) Zheng, J.; Kwak, K.; Fayer, M. D. *Acc. Chem. Res*. **2007**, *40*, 75.
(16) Cerullo, G.; Luer, L.; Manzoni, C.; De Silvestri, S.; Shoshana, O.; Ruhman, S. *J. Phys. Chem. A* **2003**, *107*, 8339.
(17) Ruhman, S.; Hou, B. X.; Friedman, N.; Ottolenghi, M.; Sheves, M. *J. Am. Chem. Soc*. **2002**, *124*, 8854.
(18) Martini, I. B.; Barthel, E. R.; Schwartz, B. J. *Science* **2001**, *293*, 462.
(19) Truong, T. V.; Shen, Y. R. *J. Chem. Phys*. **2005**, *122*, 091104.
(20) Gai, F.; McDonald, J. C.; Anfinrud, P. A. *J. Am. Chem. Soc*. **1997**, *119*, 6201.
(21) Logunov, S. L.; Volkov, V. V.; Braun, M.; El-Sayed, M. A. *Proc. Natl. Acad. Sci. U.S.A.* **2001**, *98*, 8475.
(22) Yan, M.; Rothberg, L.; Callender, R. *J. Phys. Chem. B* **2001**, *105*, 856.
(23) Wohlleben, W.; Buckup, T.; Hashimoto, H.; Cogdell, R. J.; Herek, J. L.; Motzkus, M. *J. Phys. Chem. B* **2004**, *108*, 3320.
(24) Papagiannakis, E.; Vengris, M.; Larsen, D. S.; van Stokkum, I. H. M.; Hiller, R. G.; van Grondelle, R. *J. Phys. Chem. B* **2006**, *110*, 512.
(25) Kennis, J. T. M.; Larsen, D. S.; van Stokkum, N. H. M.; Vengris, M.; van Thor, J. J.; van Grondelle, R. *Proc. Natl. Acad. Sci. U.S.A.* **2004**, *101*, 17988.
(26) Larsen, D. S.; van Stokkum, I. H. M.; Vengris, M.; van der Horst, M. A.; de Weerd, F. L.; Hellingwerf, K. J.; van Grondelle, R. *Biophys. J*. **2004**, *87*, 1858.
(27) Larsen, D. S.; Vengris, M.; van Stokkum, I. H. M.; van der Horst, M. A.; De Weerd, F. L.; Hellingwerf, K. J.; van Grondelle, R. *Biophys. J*. **2004**, *86*, 2538.
(28) Vengris, M.; van Stokkum, I. H. M.; He, X.; Bell, A. F.; Tonge, P. J.; van Grondelle, R.; Larsen, D. S. *J. Phys. Chem. A* **2004**, *108*, 4587.
(29) Larsen, D. S.; Papagiannakis, E.; van Stokkum, I. H. M.; Vengris, M.; Kennis, J. T. M.; van Grondelle, R. *Chem. Phys. Lett*. **2003**, *381*, 733.
(30) Austin, R. H.; Beeson, K. W.; Eisenstein, L.; Frauenfelder, H.; Gunsalus, I. C. *Biochemistry* **1975**, *14*, 5355.
(31) Miers, J. B.; Postlewaite, J. C.; Cowen, B. R.; Roemig, G. R.; Lee, I.-Y. S.; Dlott, D. D. *J. Chem. Phys*. **1991**, *94*, 1825.
(32) Post, F.; Doster, W.; Karvounis, G.; Settles, M. *Biophys. J*. **1993**, *64*, 1833.
(33) Agmon, N.; Doster, W.; Post, F. *Biophys. J*. **1994**, *66*, 1612.
(34) Tian, W. D.; Sage, J. T.; Champion, P. M.; Chien, E.; Sligar, S. G. *Biochemistry* **1996**, *35*, 3487.
(35) Gaab, K. M.; Bardeen, C. J. *J. Phys. Chem. A* **2004**, *108*, 10801.
(36) Gaab, K. M.; Bardeen, C. J. *Phys. Rev. Lett*. **2004**, *93*, 056001.
(37) van der Meer, M. J.; Zhang, H.; Glasbeek, M. *J. Chem. Phys*. **2000**, *112*, 2878.
(38) Changenet, P.; Zhang, H.; van der Meer, M. J.; Glasbeek, M. *J. Phys. Chem. A* **1998**, *102*, 6716.
(39) Changenet, P.; Zhang, H.; van der Meer, M. J.; Glasbeek, M.; Plaza, P.; Martin, M. M. *J. Fluoresc*. **2000**, *10*, 155.
(40) Mukamel, S. *Principles of Nonlinear Optical Spectroscopy*; Oxford University Press: New York, 1995; Vol. 6.
(41) Khurmi, C.; Berg, M. A. To be submitted for publication.
(42) Fayer, M. D. *Annu. Rev. Phys. Chem*. **1982**, *33*, 63.
(43) Trebino, R.; Barker, C. E.; Siegman, A. E. *IEEE J. Quantum Electron*. **1986**, *QE-22*, 1413.
(44) Eichler, H. J. *Laser-Induced Dynamic Gratings*; Springer: Berlin, 1986.
(45) Goodno, G. D.; Dadusc, G.; Miller, R. J. D. *J. Opt. Soc. Am. B* **1998**, *15*, 1791.
(46) Maznev, A. A.; Nelson, K. A.; Rogers, T. A. *Opt. Lett.* **1998**, *23*, 1319.
(47) Ogilvie, J. P.; Plazanet, M.; Dadusc, G.; Miller, R. J. D. *J. Phys. Chem. B* **2002**, *106*, 10460.
(48) Cowan, M. L.; Ogilvie, J. P.; Miller, R. J. D. *Chem. Phys. Lett.* **2004**, *386*, 184.
(49) Khalil, M.; Demirdoven, N.; Golonzka, O.; Fecko, C. J.; Tokmakoff, A. *J. Phys. Chem. A* **2000**, *104*, 5711.
(50) Xu, Q.-H.; Ma, Y.-Z.; Fleming, G. R. *Chem. Phys. Lett.* **2001**, *338*, 254.
(51) Qing-Hua, X.; Ying-Zhong, M.; Igor, V. S.; Graham, R. F. *J. Chem. Phys.* **2002**, *116*, 9333.
(52) Xu, Q. H.; Ma, Y. Z.; Fleming, G. R. *J. Phys. Chem. A* **2002**, *106*, 10755.
(53) Brixner, T.; Mancal, T.; Stiopkin, I. V.; Fleming, G. R. *J. Chem. Phys.* **2004**, *121*, 4221.
(54) Moran, A. M.; Nome, R. A.; Scherer, N. F. *J. Chem. Phys.* **2006**, *125*.
(55) Moran, A. M.; Nome, R. A.; Scherer, N. F. *J. Phys. Chem. A* **2006**, *110*, 10925.
(56) Khurmi, C.; Berg, M. A. To be submitted for publication.
(57) Benigno, A. J.; Ahmed, E.; Berg, M. A. *J. Chem. Phys.* **1996**, *104*, 7382.
(58) Yu, J.; Berg, M. A. *Chem. Phys. Lett.* **1993**, *208*, 315.
(59) Somoza, M. I.; Andreatta, D.; Coleman, R. S.; Murphy, C. J.; Berg, M. A. *Nucleic Acids Res.* **2004**, *32*, 2495.
(60) Kurnikova, M. G.; Balabai, N.; Waldeck, D. H.; Coalson, R. D. *J. Am. Chem. Soc.* **1998**, *120*, 6121.